Journal of the Nigerian Association of Mathematical Physics
***Volume 51 (May, 2019 Issue*), pp17 – 24**
© J. of NAMP

HEAT AND MASS TRANSFER OF A CASSON FLUID OVER AN EXPONENTIALLY PERMEABLE SHRINKING SHEET IN POROUS MEDIUM AND IN THE PRESENCE OF A MAGNETIC FIELD

E. O. Oghre[1*], I. F. Ekang[2] and A. O. Popoola[3]

[1]Department of Mathematics, Faculty of Physical Science, University of Benin, Benin City, Nigeria.
[2]Department of Mathematics, Faculty of Science, University of Uyo, Uyo, Nigeria.
[3]Department of Mathematics, Osun State University, Osogbo.

Abstract

The influence of some fluid parameters of engineering interest on heat and mass transfer of a Casson fluid over an exponentially permeable shrinking sheet in porous medium and in the presence of a magnetic field is considered. The resulting partial differential equations are converted to a system of ordinary differential equations using the appropriate similarity transformation and solved numerically using shooting technique with fourth order Runge – Kutta method. We observed that the Casson parameter, Hartmann number, permeability parameter, suction parameter, Eckert number, Prandtl number and Schmidt number are significant to the momentum and thermal boundary layer thickness, and solute concentration. Furthermore, the skin friction coefficient, heat and mass transfer coefficients are influenced by the increase in Casson and permeability parameters.
The study concludes that some fluid parameters have significant effect on the heat and mass transfer of the fluid. Graphical demonstration of the results showed more lights on the behavior of the system. An excellent agreement was also found when the results obtained in this study was compared with the previous literature.

LIST OF SYMBOLS

(x, y)	are distance along axes	p_y	is the yield stress of the fluid.
(u, v)	are components of velocities	e_{ij}	is the $(i, j)th$ component of the deformation rate
L	is the reference length	μ_B	is the plastic dynamic viscosity of Cassonfluid.
K	is the permeability of the porous medium	ϑ	is the kinematic viscosity
B_o	is the strength of the magnetic field	σ	is the electrical conductivity
q_w	is the heat flux from the sheet	R	is the reaction parameter
Pr	is the Prandtl number	λ	is the permeability parameter
Ec	is the Eckert number	τ_w	is the shear-stress along the exponentially shrinking sheet.
M	is the Hartmann number	π	is the product of the deformation rate with itself
Re	is the Reynold number	π_c	is the critical value of the product of the component of the rate of strain tensor with itself.
Sc	is the Schmidt number		

1. INTRODUCTION

The study of non-Newtonian Casson fluid has been given much priority by researchers due to its usefulness in areas of food processing, bioengineering operations and petroleum production. Casson fluid is an example of non-Newtonian fluids and behaves like elastic solids. Examples of Casson fluids are Jelly, tomato sauce, honey, etc.

Corresponding Author**:** Oghre E.O., Email: eoghre@yahoo.com, Tel: +2348033551266, +233208521257

The flow and heat transfer due to exponentially shrinking sheet were first considered [1] and the effect of magnetic field was experimented [2]. Casson fluid flow and heat transfer over a nonlinearly stretching surface was investigated [3]. Heat transfer over an exponentially stretching continuous surface with suction was examined [4].Heat transfer in boundary layer flow of a Casson fluid over a permeable shrinking sheet with viscous dissipation was studied [5].Dual solution of non-Newtonian Casson fluid flow and heat transfer over an exponentially permeable shrinking sheet with viscous dissipation was considered [6].The flow due to shrinking sheet was introduced [7], and [8] established that for steady flow due to shrinking sheet, certain amount of wall mass suction is required to restrain the generated vorticity. Analytic solution for MHD boundary layer flow of Casson fluid over a stretching/shrinking sheet with wall mass transfer and their study revealed that magnetic field influences the behaviour of the flow dynamics was studied [9]. The effects of mass transfer on MHD flow of Casson fluid with chemical reaction and suction was examined [10].The diffusion of chemically reactive species of a Casson fluid flow over an exponentially stretching surface was investigated [11].Diffusion of chemically reactive species in Casson fluid flow over an unsteady stretching surface in porous medium in the presence of a magnetic field was studied [12]. Heat and mass transfer in MHD Casson fluid over an exponentially permeable stretching surface was examined [13]. Heat and mass transfer in hydromagnetic radiative Casson fluid flow over an exponentially stretching sheet with heat source/sink was investigated [14]. Casson fluid flow in a piped filled with homogeneous porous medium was studied [15].Flow and heat transfer of Casson fluid from a horizontal circular cylinder with partial slip in non-Darcy porous medium was examined [16]. In this work, we extended the work of [6] in which the mass equation, the source terms for porous medium and magnetic fields are introduced. Similarity transformation are employed to transform the governing partial differential equations into non-linear ordinary differential equations which are solved numerically using shooting technique with fourth order Runge-Kutta method. The effect of Casson parameter, Hartmann number, permeability parameter, suction parameter, Eckert number, Prandtl number, Schmidt number were examined and discussed.

2. MATHEMATICAL FORMULATION

Consider a steady two-dimensional incompressible fluid flow, heat and mass transfer of a Casson fluid flow over an exponentially permeable shrinking sheet in porous medium with viscous dissipation and in the presence of a magnetic field. The sheet is situated at $y = 0$, with the flow being confined in $y > 0$. The rheological equation of state for an isotropic and incompressible flow of a non-Newtonian casson fluid is written as:

$$\tau_{ij} = \begin{cases} (\mu_B + \frac{p_y}{\sqrt{2\pi}})2e_{ij}; \pi \rangle \pi_c \\ (\mu_B + \frac{p_y}{\sqrt{2\pi_c}})2e_{ij}; \pi \langle \pi_c \end{cases}$$

Where $\pi = e_{ij}e_{ji}$

$$e_{ij} = \frac{1}{2}(\frac{\partial u_i}{\partial x_j} + \frac{\partial u_j}{\partial x_i}) \qquad . \qquad . \qquad (1)$$

The following assumptions were made before deriving the governing equations. We introduced the source term for porous medium, magnetic field and the mass equation. Temperature and concentration of the fluid at the wall are raised to T_w and C_w respectively and are greater than the ambient temperature and concentration of the fluid, T_∞ and C_∞ respectively.

The temperature, T_w and concentration, C_w at the surface are given by

$$T_w(x) = T_\infty + be^{\frac{2x}{L}}$$

$$C_w(x) = C_\infty + ce^{\frac{2x}{L}} \qquad . \qquad . \qquad (2)$$

where T_∞, C_∞, b and c are constants.

By these assumptions the governing equations are as follows;

$$\frac{\partial u}{\partial x} + \frac{\partial v}{\partial y} = 0$$

$$u\frac{\partial u}{\partial x} + v\frac{\partial u}{\partial y} = \vartheta(1+\frac{1}{\beta})\frac{\partial^2 u}{\partial y^2} - \frac{\vartheta}{K}u - \frac{\sigma B_o^2}{\rho}u$$

$$u\frac{\partial T}{\partial x} + v\frac{\partial T}{\partial y} = \alpha\frac{\partial^2 T}{\partial y^2} + \frac{\vartheta}{C_p}(1+\frac{1}{\beta})(\frac{\partial u}{\partial y})^2$$

$$u\frac{\partial C}{\partial x}+v\frac{\partial C}{\partial y}=D\frac{\partial^2 C}{\partial y^2}-k_2(C-C_\infty) \qquad . \qquad . \qquad (3)$$

With boundary conditions

$$u=-u_w=-ae^{\frac{x}{L}}$$

$$v=v_o e^{\frac{x}{2L}}$$

$$T=T_w(x)=T_\infty+be^{\frac{2x}{L}}$$

$$C=C_w(x)=C_\infty+ce^{\frac{2x}{L}} \quad \text{at } y=0$$

$$\left.\begin{array}{l} u\to 0 \\ T\to T_\infty \\ C\to C_\infty \end{array}\right\} \quad \text{as } y\to\infty \qquad . \qquad . \qquad (4)$$

Where α , C_p , D are thermal diffusivity, specific heat, molecular mass diffusivity

$$\beta=\frac{\mu_B\sqrt{2\pi_c}}{p_y}$$

$$k_2=k_o e^{\frac{x}{L}} \qquad . \qquad . \qquad (5)$$

Where k_2 is the exponential reaction rate; k_2 >0 is for destructive reaction, k_2 < 0 is for constructive reaction and k_0 is a constant.

Introducing the dimensionless form:

The stream function, ψ, is defined as

$$u=\frac{\partial\psi}{\partial y} \quad \text{and} \quad v=-\frac{\partial\psi}{\partial x}$$

$$\psi=(2L\vartheta u_w)^{\frac{1}{2}}f(\eta)$$

$$=(2L\vartheta a)^{\frac{1}{2}}e^{\frac{x}{2L}}f(\eta)$$

$$\eta=(\frac{u_w}{2L\vartheta})^{\frac{1}{2}}y=(\frac{ae^{\frac{x}{L}}}{2L\vartheta})^{\frac{1}{2}}y \qquad . \qquad . \qquad (6)$$

Substituting this transformation leads to the non-dimensional flow equations

$$(1+\frac{1}{\beta})f'''+ff''-2f'^2-(\lambda+M)f'=0$$

$$\frac{1}{\Pr}\theta''+f\theta'-4f'\theta+Ec(1+\frac{1}{\beta})f''^2=0$$

$$\frac{1}{Sc}\phi''+f\phi'-4f'\phi-R\phi=0 \qquad . \qquad . \qquad (7)$$

Subject to the boundary conditions:

At $y=0$, $u=-u_w=-ae^{\frac{x}{L}}$ implies $\eta=0$

But $u=ae^{\frac{x}{L}}f'(\eta)$

$$f'(0)=-1$$

$$f(0)=-V_o(\frac{2L}{a\vartheta})=S>0$$

$$\theta(0)=1$$

$$\phi(0)=1$$

$$\left.\begin{aligned} f'(\eta) &\to 0 \\ \theta'(\eta) &\to 0 \\ \phi'(\eta) &\to 0 \end{aligned}\right\} \text{ as } \eta \to \infty \quad . \qquad . \qquad (8)$$

The quantities of engineering interest are the local skill friction coefficient, the Nusselt and Sherwood numbers which are defined as:

$$C_f = \frac{\tau_w}{\rho u_w^2}$$

$$Nu_x = \frac{x q_w}{K_1 (T_w - T_\infty)}$$

$$Sh_x = \frac{x}{D} \cdot \frac{J_w}{(C_w - C_\infty)}$$

$$C_f \operatorname{Re}_x^{\frac{1}{2}} \left(\frac{2L}{x}\right)^{1/2} = (1 + \frac{1}{\beta}) f''(0)$$

$$Nu_x \operatorname{Re}_x^{-\frac{1}{2}} (\frac{2L}{x})^{\frac{1}{2}} = -\theta'(0)$$

$$Sh_x = -(\frac{x}{2L})^{\frac{1}{2}} \operatorname{Re}_x^{\frac{1}{2}} \phi'(0) \quad . \qquad . \qquad (9)$$

Where $\operatorname{Re}_x = \frac{x u_w}{\vartheta} \to$ Local Reynolds Number.

The system of equations (7) reduces to those of[6] when λ=M=Sc=0.

The equations (7) and (8) are solved numerically using shooting technique with fourth order Runge-Kutta method. The boundary condition as $\eta \to \infty$ was replaced by a finite value inaccordance with standard practice in boundary layer analysis. We set $\eta_\infty = 10$.

3. RESULTS AND DISCUSSION

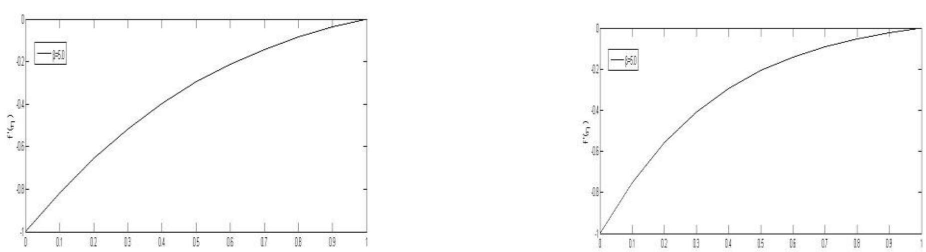

(a) (b)

Figure 1: A comparison of velocity profiles 0f (a) [6] when M=Sc=R=**λ**=0 and (b) present study.

To have a clear knowledge of Casson fluid flow, we analyse the effects of the fluid parameters on $f'(\eta), \theta(\eta)$ and $\phi(\eta)$. The variation of $f''(0)$, $-\theta'(0)$ and $-\phi'(0)$ with suction parameter (S) varying β and λ are shown.

To validate the numerical method used in this work, the results for the velocity profiles were compared to that of [6] at Casson parameter, β=5.0, for the fluid parameter M=λ=Sc=R=O. The comparison is shown in figure 1 [(a) and (b)].

A comprehensive numerical calculation is computed for different fluid parameters and the results are displayed through figures 2 – 7 for $f'(\eta), \theta(\eta)$ and $\phi(\eta)$.

In figures 2(a), 3(a), 4(a), increasing the Casson parameter increases the velocity profiles and the boundary layer thickness reduces. The Casson parameter produces a resistance in the fluid flow and consequently the boundary layer thickness decreases for higher value of Casson parameter. For various Casson parameters, it is noted that the temperature of the fluid decreases and reduces the thermal boundary layer thickness. This is due to the fact that the introduction of tensile stress due to elasticity leads to contraction in the boundary layer thickness. The solute concentration for both destruction and construction decrease with increasing values of Casson parameters.

In figures 2(b), 3(f), 4(e), increasing the Hartmann number increases the velocity profiles and decreases the temperature profiles leading to the transfer of heat. The solute concentration for both destruction and construction decrease with increasing values of Hartmann numbers.
In figures 2(c), 3(e), 4(b), increasing permeability parameter enhances the velocity profiles and reduces temperature and concentration profiles leading to the transfer of heat and reduction of the solute concentration.
In figures 2(d), 3(d), 4(d), increasing the suction parameter increases the velocity and temperature profiles. Increasing the Schmidt number (in figure 3(c)) and the suction parameter decreases the solute concentration for destructive reaction and increases the solute concentration for constructive reaction. The suction parameter is to maintain the steady flow near the sheet by delaying the separation. The solute boundary layer increases when R<0, that is, constructive reaction and decrease when R>0, that is, destructive reaction.
In figures 3(b), 4(c), increasing the Prandtl and Eckert numbers enhances fluid thermal conductivity which in turns causes an increase in thermal boundary layer thickness. More heat is generated in the boundary layer region due to the viscous dissipation and hence it increases the heat transfer rate from the hot sheet to the ambient fluid.
In figures 5(a&b), 6(a&b), 7(a&b), increasing Casson and permeability parameters decreases the skin friction coefficient but at S = 2.316, there is a stability and for S > 2.316, the skin friction coefficient increases. Increasing Casson parameters increases the heat transfer coefficient and increasing permeability parameter decreases the heat transfer coefficient. Increasing Casson parameter increases the mass transfer coefficient and increasing permeability parameter decreases the mass transfer coefficient.

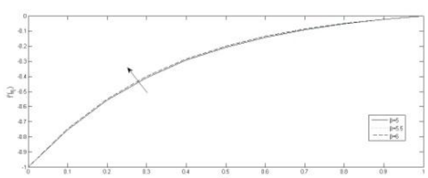

(a) Influence of β on $f'(\eta)$

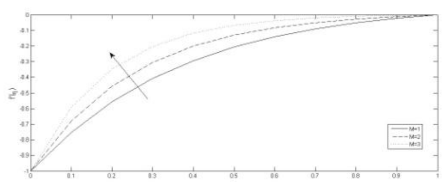

(b) Influence of M on $f'(\eta)$

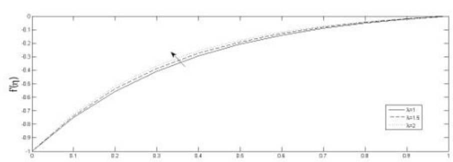

(c) Influence of λ on $f'(\eta)$

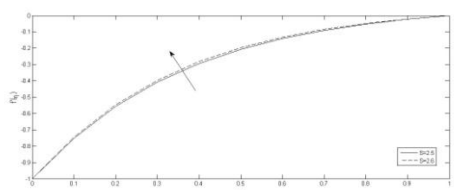

(d) Influence of S on $f'(\eta)$

Figure 2: Computational results for velocity profiles.

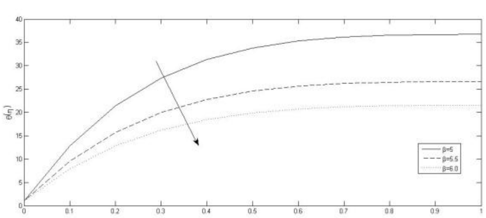

(a) Influence of β on $\theta(\eta)$

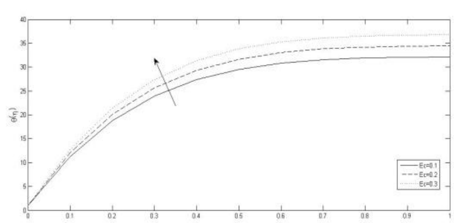

(b)Influence of Ec on $\theta(\eta)$

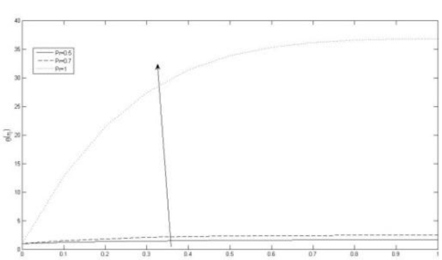

(c) Influence of Pr on $\theta(\eta)$

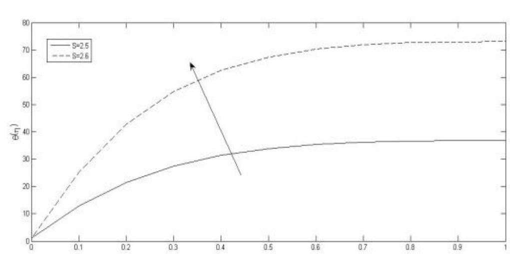

(d) Influence of S on $\theta(\eta)$

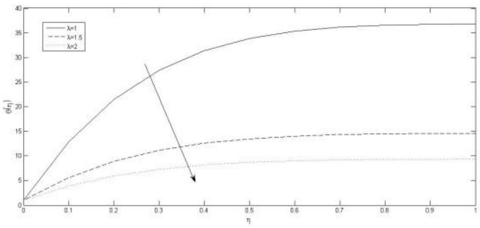

(e) Influence of λ on $\theta(\eta)$

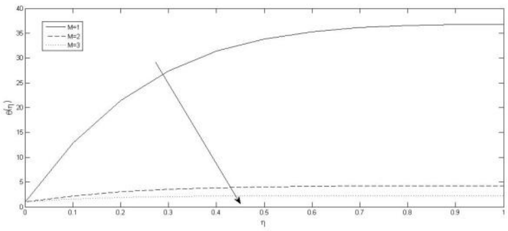

(f) Influence of M on $\theta(\eta)$

Figure 3: Computational results for temperature profiles.

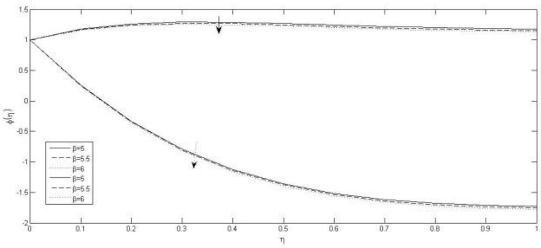

(a) Influence of β on $\phi(\eta)$ with destruction and construction respectively.

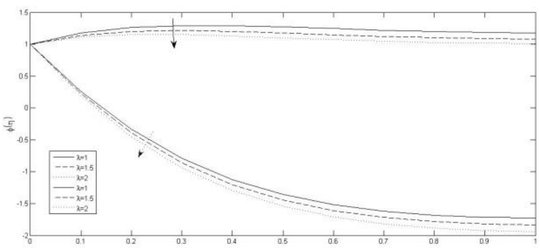

(b) Influence of λ on $\phi(\eta)$ with destruction and construction respectively.

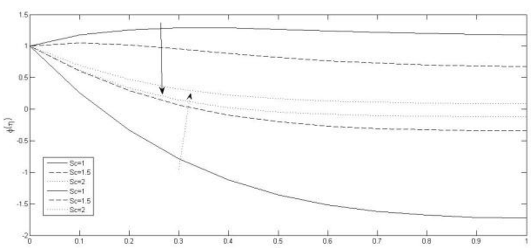

(c) Influence of Sc on $\phi(\eta)$ with destruction and construction respectively.

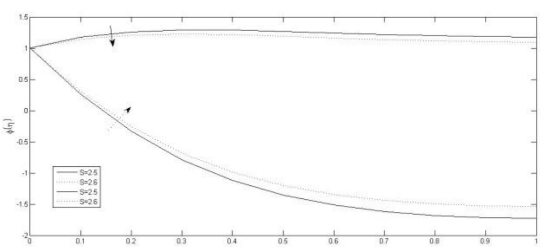

(d) Influence of S on $\phi(\eta)$ with destruction and construction respectively.

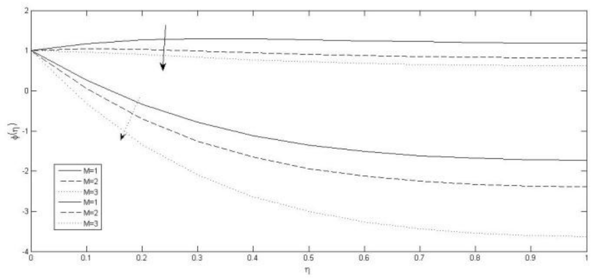

(e) Influence of M on $\phi(\eta)$ with destruction and construction respectively.

Figure 4: Computational results for concentration profiles.

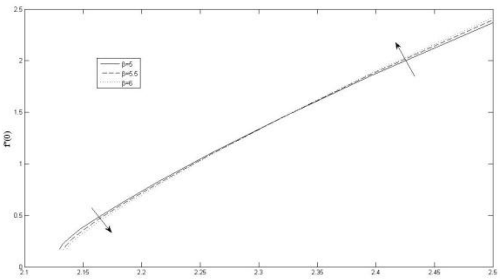

(a) Influence of β on $f''(0)$ with S.

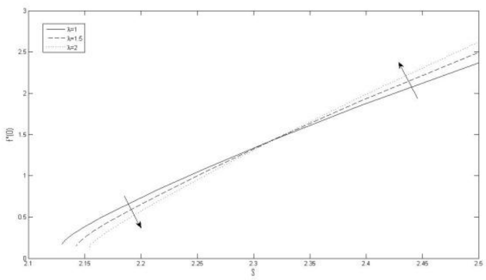

(b) Influence of λ on $f''(0)$ with S.

Figure 5: Computational results for skin friction coefficients.

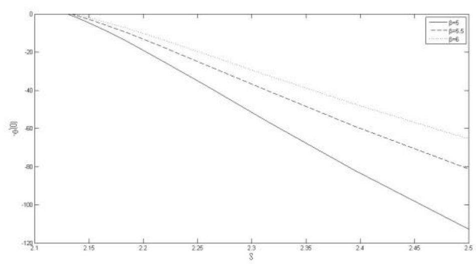

(a) Influence of β on -$\theta'(0)$ with S.

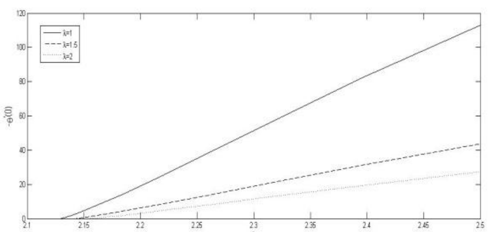

(b) Influence of λ on -$\theta'(0)$ with S.

Figure 6: Computational results for heat transfer coefficients.

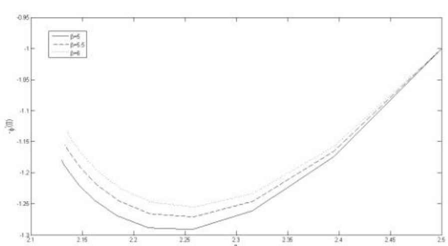

(a) Influence of β on $-\phi'(0)$ with S.

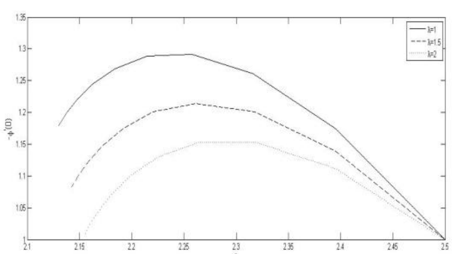

(b) Influence of λ on $-\phi'(0)$ with S.

Figure 7: Computational results for mass transfer coefficients.

4. CONCLUSION

Heat and mass transfer of steady boundary layer of a Casson fluid flow over a permeability exponentially shrinking sheet in a porous medium with viscous dissipation and in the presence of a magnetic field are studied. The governing equations are solved as stated earlier.

The following conclusions are made:

i. The momentum boundary layer thickness increases with β, M, **λ** and S.
ii. The thermal boundary layer thickness decreases with increased in β, M, **λ** and increases with Ec, Pr and S.
iii. The solute concentration for destructive reaction decreases with increased in the Casson parameter, suction parameter, Hartmann number, Schmidt number, permeability parameter whereas the solute concentration for constructive reaction decreases with increasing Casson parameter, Hartmann number, permeability parameter and increases with suction parameter and Schmidt number.
iv. The heat and mass transfer coefficients increase with Casson parameter and decreases with increased in permeability parameter. The skin friction coefficient has a stability at S=2.316, decreases with increased in Casson parameter and permeability parameter when S<2.316, and increases with Casson parameter and permeability parameter when S>2.316.

REFERENCES

[1] Bhattacharya, K. (2011), “Boundary Layer Flow and Heat Transfer over an Exponentially Shrinking Sheet”, Chinese Physics Letters, Vol. 28, no. 7, Article ID 074701.
[2] Bhattacharyya, K. and Pop, I. (2011), “MHD Boundary Layer Flow due to an Exponentially Shrinking Sheet”, Magnetohydrodynamics, vol. 47, no. 4, pp. 337-344.
[3] Mukhopadhyay, S. (2013), “Casson Fluid Flows and Heat Transfer over a nonlinearly Stretching Surface,” Chin Phys. B, Vol. 22, no. 7, Article ID 074701.
[4] Elbashbeshy, E. M. A. (2001), “Heat Transfer over an Exponentially Stretching Continuous Surface with Suction”, Archives of Mechanics, vol. 53, no. 6., pp. 643-651.
[5] Qasim, M. and Noreen, S. (2014), “Heat Transfer in the Boundary Layer Flow of a Casson Fluid over a Permeable Shrinking Sheet with Viscous Dissipation”, The European Physical Journal Plus, vol. 129, Article 7.
[6] Zaib, A., Bhattacharyya, K., Uddiri, M. S. and Shafie, S. (2016), “Dual Solution of Non -Newtonian Casson Fluid Flow and Heat Transfer over an Exponentially Permeable Shrinking Sheet with Viscous Dissipation”, Hindawi Publishing Corporation, Modelling and Simulation in Engineering, vol. 2016, Article ID 6968371, 8 pages.
[7] Wang, C. Y. (1990), “Liquid film on an Unsteady Stretching Sheet”, Quartely of Applied Mathematics, Vol.48, pp.601-610.
[8] Miklavcic, M. and Wang, C. Y. (2006), “Viscous flow due to a Shrinking Sheet”, Quarterly of Applied Mathematics, Vol.64, no.2, pp.283-290.
[9] Bhattacharyya, K., Hayat, T. and Alsaedi, A. (2013), “Analytic Solution for MHD Boundary Sheet with Casson Fluids over a Stretching/Shrinking Sheet with Wall Mass Transfer”, Chinese Physics B, vol. 22, no. 2, Article ID 024702.
[10] Shehzad, S. A., Hayat, T., Qasim, M. and Asghar, S. (2013), “Effect of Mass Transfer an MHD flow of Casson Fluid with Chemical Reaction and Suction”, Brazilian Journal of Chemical Engineering, vol. 30, no. 01, pp. 187-195.
[11] Mukhopadhayay, S. and Gorla, R. S. R. (2014), “Diffusion of Chemically Reactive Species of a Casson Fluid flow over an Exponentially Stretching Surface”, TEPE, vol. 3, no.2, pp. 216-221.
[12] Makanda, G., Shaw, S. and Sibanda, P. (2015), “Diffusion of Chemically Reactive Species in Casson Fluid flow over an Unsteady Stretching Surface in Porous Medium in the Presence of a Magnetic Field”, Hindawi publishing corporation, Mathematical Problems in Engineering, Vol. 2015, Article ID 724596, 10 pages.
[13] Raju, C. S. K., Sugunamma, V., Babu, M. J., Reddy, J. V. R. (2016), “Heat and Mass Transfer in Magnetohydrodynamic Casson Fluid over an Exponentially Permeable Stretching Surface”, Engineering Science and Technology, an International Journal,19, 45-52.
[14] Prakash, J., Prasad, P. D., Kumar, G. V., Kumar, R. V. M. S. S. K. and Varma, S. V. K. (2016), “Heat and Mass Transfer in Hydromagnetic Radiation Casson Fluid Flow over an Exponentially Stretching Sheet with Heat Source/Sink”, International Journal of Engineering Science Invention, Vol. 5, Issue 7, pp. 12-23.
[15] Dash, R. K., Mehta, K. N. and Jayaraman, G. (1996), “Casson Fluid Flow in a Pipe filled with a Homogeneous Porous Medium”, International Journal of Engineering Science, Vol. 34, pp. 1145-1156.
[16] Ramachandra, P. V., Subba, R. A. and Anwar, B. O. (2013), “Flow and Heat Transfer of Casson Fluid from a Horizontal Circular Cylinder with Partial Slip in non-Darcy Porous Medium”, Journal of Applied and computational mathematics, 2.2.